2,4-Ethanotetraborane Derivatives. 2.[1] Synthesis, Characterization, and Gas-Phase Structures of 2,4-(MeCHCH$_2$)B$_4$H$_8$, 2,4-(*trans*-MeCHCHMe)B$_4$H$_8$, and 2- and 4-Pr-2,4-(MeCHCH$_2$)B$_4$H$_7$

Paul T. Brain,[†] Michael Bühl,[‡] Mark A. Fox,[§] Robert Greatrex,*[,§] Ellen Leuschner,[§] Matthew J. Picton,[†] David W. H. Rankin,*[,†] and Heather E. Robertson[†]

Department of Chemistry, University of Edinburgh, West Mains Road, Edinburgh, EH9 3JJ, U.K., Institut für Organische Chemische, Universität der Zürich, Winterthurerstrasse 190, CH-8057, Zürich, Switzerland, and School of Chemistry, University of Leeds, Leeds, LS2 9JT, U.K.

Received December 29, 1994[⊗]

The compounds 2,4-(methylethano)tetraborane(10), (MeCHCH$_2$)B$_4$H$_8$ (**1**), and 2,4-(*trans*-dimethylethano)-tetraborane(10), (MeCHCHMe)B$_4$H$_8$ (**2**), synthesized from B$_4$H$_{10}$ and MeCH=CH$_2$ or *trans*-MeCH=CHMe, respectively, have been characterized and their molecular structures determined by gas-phase electron diffraction and *ab initio* computations at the MP2/6-31G* level. The equilibrium structures of 2- and 4-*n*-propyl-2,4-(methylethano)tetraborane, 2-Pr-2,4-(MeCHCH$_2$)B$_4$H$_7$ (**3**) and 4-Pr-2,4-(MeCHCH$_2$)B$_4$H$_7$ (**4**), obtained as side products in the synthesis of **1**, have also been characterized and their structures optimized using *ab initio* computations. **3** and **4** represent the first examples of trisubstituted derivatives of tetraborane(10). The diffraction patterns of **1** and **2** are consistent with heavy-atom, C$_2$B$_4$, cages that are only slightly distorted away from C_{2v} symmetry with twist angles of 0.5 and 0.8°, respectively, for the C(5)−C(6) bonds about the pseudo-C_2 axis. Other structural parameters (r_a) of the experimental geometries for 2,4-(MeCHCH$_2$)B$_4$H$_8$ and 2,4-(MeCHCHMe)-B$_4$H$_8$, respectively, include *r*[B(1)−B(2] (hinge−wing) = 189.1(2) and 189.3(3), *r*[B(1)−B(3)] (hinge−hinge) = 171.6(8) and 171.2(9), *r*(B−C) = 161.2(9) and 161.5(11), and *r*(C−C) (skeleton) = 156.2(9) and 156.7(11) pm; B(1)B(2)B(3) = 54.0(2) and 53.7(3)°, and the dihedral ("butterfly") angles between the planes B(1)B(2)B(3) and B(1)B(4)B(3) are 100.4(2) and 100.4(3)°. These values agree well with the *ab initio* (MP2/6-31G* level) optimized molecular geometries and are supported by comparison of the calculated (IGLO) ^{11}B NMR chemical shifts, using both the MP2/6-31G* and GED geometries, with the experimental NMR data. The theoretical structures of **3** and **4** are also supported by ^{11}B NMR chemical-shift calculations.

Introduction

The use of the combined *ab initio*/IGLO/NMR method[1−7] to augment and/or support the determination of gas-phase structures by electron diffraction has proved to be very successful, especially for relatively small boranes.[1,6,7] In this approach, various structures derived from experiment and from *ab initio* geometry optimizations are assessed by means of IGLO (individual gauge for localized orbitals)[5] NMR calculations. The ^{11}B chemical shifts obtained by this method for various geometries are compared with the experimental chemical shifts. Using geometries optimized at electron-correlated levels of theory (*e.g.* MP2/6-31G*, *i.e.* with a basis set including polarization functions), the agreement between experimental and IGLO ^{11}B chemical shifts has been found to be consistently good.[2a]

In electron-diffraction analyses, the parameters defining the structures of boranes, especially those for the boron framework, are often subject to significant correlation.[6,7] Moreover, it is possible that several geometries will fit the electron-scattering data more or less equally well and additional information (*e.g.* spectroscopic or theoretical) is required to decide which of the options is correct.[8] Whenever it is feasible, therefore, we perform both experimental and theoretical work, so that the results obtained are as reliable as possible.

Recently, we have reported the structural characterization of 2,4-ethanotetraborane(10), (CH$_2$CH$_2$)B$_4$H$_8$, more commonly known as dimethylenetetraborane.[1] This was synthesized *via* the reaction of B$_4$H$_{10}$ with ethene and consists of a tetraborane "butterfly" cage substituted at the "wing" B(2) and B(4) atoms

* Authors to whom correspondence should be addressed.
[†] University of Edinburgh.
[‡] Universität der Zürich.
[§] University of Leeds.
[⊗] Abstract published in *Advance ACS Abstracts,* May 1, 1995.

(1) For part 1 see: Hnyk, D.; Brain, P. T.; Rankin, D. W. H.; Robertson, H. E.; Greatrex, R.; Greenwood, N. N.; Kirk, M.; Bühl, M.; Schleyer, P. v. R. *Inorg. Chem.* **1994**, *33*, 2572.
(2) (a) Bühl, M.; Schleyer, P. v. R. *J. Am. Chem. Soc.* **1992**, *114*, 477. (b) Bühl, M.; Schleyer, P. v. R. In *Electron Deficient Boron and Carbon Clusters*; Olah, G. A., Wade, K., Williams, R. E., Eds.; Wiley: New York, 1991; Chapter 4, p 113.
(3) (a) Schleyer, P. v. R.; Bühl, M.; Fleischer, U.; Koch, W. *Inorg. Chem.* **1990**, *29*, 153. (b) Bühl, M.; Schleyer, P. v. R. *Angew. Chem., Int. Ed. Engl.* **1990**, *29*, 886.
(4) For other examples, see: (a) Hnyk, D.; Vajda, E.; Bühl, M.; Schleyer, P. v. R. *Inorg. Chem.* **1992**, *31*, 2464. (b) Mebel, A. M.; Charkin, O. P.; Bühl, M.; Schleyer, P. v. R. *Inorg. Chem.* **1993**, *32*, 463. (c) Onak, T.; Tseng, J.; Diaz, M.; Tran, D.; Arias, J.; Herrera, S.; Brown, D. *Inorg. Chem.* **1993**, *32*, 487.
(5) (a) Kutzelnigg, W. *Isr. J. Chem.* **1980**, *19*, 193. (b) Schindler, M.; Kutzelnigg, W. *J. Chem. Phys.* **1982**, *76*, 1919. (c) Review: Kutzelnigg, W.; Fleischer, U.; Schindler, M. In *NMR, Basic Principles and Progress*; Springer Verlag: Berlin, 1990; Vol. 23, p 165. (d) Meier, U.; van Wüllen, C.; Schindler, M. *J. Comput. Chem.* **1992**, *13*, 551.
(6) Brain, P. T.; Hnyk, D.; Rankin, D. W. H.; Bühl, M.; Schleyer, P. v. R. *Polyhedron* **1994**, *13*, 1453.
(7) Brain, P. T.; Rankin, D. W. H.; Robertson, H. E.; Alberts, I. L.; Schleyer, P. v. R.; Hofmann, M. *Inorg. Chem.* **1994**, *33*, 2565.
(8) For example, see: (a) Hargittai, I., Hargittai, M., Eds. *Stereochemical Applications of Gas-Phase Electron Diffraction, Part A*; VCH: Weinheim, Germany, 1990; p 301. (b) Hnyk, D.; Bühl, M.; Schleyer, P. v. R.; Volden, H. V.; Gundersen, S.; Müller, J.; Paetzold, P. *Inorg. Chem.* **1993**, *32*, 2442.

0020-1669/95/1334-2841$09.00/0

Table 1. Nozzle-to-Plate Distances (mm), Weighting Functions (nm^{-1}), Correlation Parameters, Scale Factors, and Electron Wavelengths (pm)

molecule	nozzle-to-plate dist	Δs	s_{min}	sw_1	sw_2	s_{max}	correlation param	scale factor, k^a	electron wavelength[b]
2,4-(MeCHCH$_2$)B$_4$H$_8$	258.31	2	20	40	140	164	0.429	0.681(10)	5.704
	200.48	4	40	60	192	224	−0.225	0.796(12)	5.692
2,4-(MeCHCHMe)B$_4$H$_8$	258.25	2	20	40	136	160	0.473	0.667(7)	5.692
	200.07	4	40	60	192	224	−0.259	0.745(9)	5.704

[a] Figures in parentheses are the estimated standard deviations. [b] Determined by reference to the scattering pattern of benzene vapor.

by a bridging C_2H_4 moiety giving C_{2v} symmetry, overall.[1,9,10] Derivatives of ethanotetraborane have been reported by Onak *et al.*, *viz.* 2,4-(MeCHCH$_2$)B$_4$H$_8$ and 2,4-(MeCHCHMe)B$_4$H$_8$;[10] these were also obtained from B$_4$H$_{10}$ by reaction with MeCH=CH$_2$ or H$_2$C=C=CH$_2$ for the former and *trans*- or *cis*-MeCH=CHMe for the latter derivative. The NMR data of these suggested that (i) the cage strain is accommodated mainly at the carbon atoms by enlargement of one or more BCC bond angles and (ii) the MeCH−CH$_2$ or MeCH−CHMe groups of the BCCB bridges are slightly staggered.[10]

We present here the results of a study of the reactions of B$_4$H$_{10}$ with MeCH=CH$_2$ and B$_4$H$_{10}$ with *trans*-MeCH=CHMe. 2,4-(MeCHCH$_2$)B$_4$H$_8$ (**1**), 2-Pr-(MeCHCH$_2$)B$_4$H$_7$ (**3**), and 4-Pr-2,4-(MeCHCH$_2$)B$_4$H$_7$ (**4**) (Pr = *n*-propyl) were obtained with MeCH=CH$_2$ and 2,4-(*trans*-MeCHCHMe)B$_4$H$_8$ (**2**) was obtained with *trans*-MeCH=CHMe, respectively. The electron-scattering patterns of **1** and **2** have been analyzed, and the refined structures are found to be in good agreement with the geometries obtained by the *ab initio* study. The accuracy of the structures is further substantiated by *ab initio* energy and ^{11}B chemical-shift calculations. The structures of **3** and **4** were optimized by *ab initio* computations and are supported by comparison of the experimental and calculated ^{11}B NMR chemical shifts.

Experimental Section

Synthesis. All manipulations were carried out at Leeds by employing standard high-vacuum line systems equipped with Young's greaseless O-ring taps and spherical joints. Tetraborane(10), B$_4$H$_{10}$, was obtained from Me$_4$NB$_3$H$_8$ (Alfa) and BF$_3$ (Aldrich).[11] Propene and *trans*-2-butene were obtained commercially (Matheson).

B$_4$H$_{10}$ (3 mmol) and propene (3 mmol) were mixed in a 650 mL hot−cold reactor[9] with hot/cold temperatures of 100/0 °C for 1 h. The volatiles were separated by low-temperature fractional distillation with mass spectrometric monitoring. The two volatile fractions **1** (mass cut off *m/z* 94: yield, based on B$_4$H$_{10}$ consumed, *ca.* 90%) and a mixture of **3** and **4** (*m/z* 136: yield *ca.* 4%) were collected and characterized by ^{11}B and ^{1}H NMR spectroscopy. The reaction of tetraborane(10) (3 mmol) and *trans*-2-butene (3 mmol) was carried out similarly, and **2** (*m/z* 108: yield *ca.* 86%) was collected.

Boron-11 and proton NMR spectra were recorded on a Bruker AM400 instrument (128 MHz ^{11}B and 400 MHz ^{1}H) in CDCl$_3$ at 223 K. Boron assignments were determined by comparison with IGLO calculated chemical shifts. The proton assignments were determined using ^{1}H{^{11}B selective} spectroscopy and, for C*H* in **1**, **3**, and **4**, by comparison with the $\delta(^1H)$ IGLO values.[12]

1. ^{11}B NMR (CDCl$_3$, ppm): 4.8 (d, 1B, J_{BHt} = 141 Hz; B2), 2.0 (d, 1B, J_{BHt} = 136; B4), −39.6 (m, 1B; B1), −40.9 (m, 1B; B3). ^{1}H NMR: 3.11 (q, 2H, J_{BHt} = 132; B2H, B4H), 1.31 (q, 2H, J_{BHt} = 148; B1H, B3H), 1.01 (s, 1H; MeCH or CH6), 0.92 (s, 4H; CH$_3$, MeCH or CH6), −0.03 (d, 1H, J_{HCH} = 12; CH7), −1.01 (q, 3H, $J_{BH\mu}$ = 51; H$_\mu$(1,2), H$_\mu$(3,4), H$_\mu$(1,4)), −1.32 (q, 1H, $J_{BH\mu}$ = 52; H$_\mu$(2,3)).

2. ^{11}B NMR (CDCl$_3$, ppm): 4.3 (d, 2B, J_{BHt} = 149 Hz; B2, B4), −40.1 (dt, 2B, J_{BHt} = 147, $J_{BH\mu}$ = 55; B1, B3). ^{1}H NMR: 3.01 (q, 2H, J_{BHt} = 130; B2H, B4H), 1.27 (q, 2H, J_{BHt} = 146; B1H, B3H), 0.91 (s, 6H; CH$_3$), 0.35 (s, 2H; CH), −0.86 (q, 2H, $J_{BH\mu}$ = 51; H$_\mu$(1,2), H$_\mu$(3,4)), −1.35 (q, 2H, $J_{BH\mu}$ = 50; H$_\mu$(2,3), H$_\mu$(1,4)).

3. ^{11}B NMR (CDCl$_3$, ppm): 21.9 (s, 1B; B2), −1.6 (d, 1B, J_{BHt} = 136; B4), −38.6 (m, 1B; B1), −38.9 (m, 1B; B3). ^{1}H{^{11}B} NMR: 3.00 (s, 1H; B4H), 1.36 (s, 2H; B1H, B3H), 1.5−0.8 (m, 12H; alkyl CH, CH6), 0.03 (d, 1H, J_{HCH} = 12; CH7), −0.46 (s, 1H; H$_\mu$(1,2)), −0.82 (s, 3H; H$_\mu$(3,4), H$_\mu$(1,4), H$_\mu$(2,3)).

4. ^{11}B NMR (CDCl$_3$, ppm): 19.5 (s, 1B; B4), 1.4 (d, 1B, J_{BHt} = 131; B2), −38.6 (m, 1B; B1), −38.9 (m, 1B; B3). ^{1}H{^{11}B} NMR: 3.00 (s, 1H; B2H), 1.36 (s, 2H; B1H, B3H), 1.5−0.8 (m, 12H; alkyl CH, CH6), 0.03 (d, 1H, J_{HCH} = 12; CH7), −0.46 (s, 2H; H$_\mu$(1,4), H$_\mu$(3,4)), −0.82 (s, 1H; H$_\mu$(1,2)), −1.23 (s, 1H; H$_\mu$(2,3)).

Electron-Diffraction Measurements. Electron-scattering intensities were recorded on Kodak Electron Image plates using the Edinburgh gas-diffraction apparatus operating at *ca.* 44.5 kV (electron wavelength *ca.* 5.7 pm).[13] Nozzle-to-plate distances for the all-glass inlet nozzle[14] employed were *ca.* 200 and 258 mm, yielding data in the *s* range 20−224 nm^{-1}; for **1** three long- and two medium-camera plates and for **2** four long- and three medium-camera plates were obtained and selected for analysis. The samples and nozzle were held at *ca.* 293 K during the exposure periods.

The scattering patterns of benzene were also recorded for the purpose of calibration; these were analyzed in exactly the same way as those of the tetraborane(10) derivatives so as to minimize systematic errors in the wavelengths and camera distances. Nozzle-to-plate distances, weighting functions used to set up the off-diagonal weight matrix, correlation parameters, final scale factors, and electron wavelengths for the measurements are collected together in Table 1.

The electron-scattering patterns were converted into digital form using a computer-controlled Joyce-Loebl MDM6 microdensitometer with a scanning program described elsewhere.[15] The programs used for data reduction[15] and least-squares refinement[16] have been described previously; the complex scattering factors employed were those listed by Ross *et al.*[17]

Theoretical Calculations. *Ab initio* computations employed standard procedures and basis sets[18] using the Gaussian92 program.[19] NMR chemical shifts have been calculated using the IGLO method[5] employing a Huzinaga basis set[20] of II′ quality;[5c] this is of triple-ζ plus polarization (TZP) quality for B and C and employes a double-ζ (DZ)

(9) Harrison, B. C.; Solomon, I. J.; Hites, R. D.; Klein, M. J. *J. Inorg. Nucl. Chem.* **1960**, *14*, 195.
(10) Onak, T.; Gross, K.; Tse, J.; Howard, J. *J. Chem. Soc., Dalton Trans.* **1973**, 2633.
(11) Toft, M. A.; Leach, J. B.; Himpsl, F. L.; Shore, S. G. *Inorg. Chem.* **1982**, *21*, 1952.
(12) At the II//MP2/6-31G* level, the chemical shifts for the C*H* protons of **1** are calculated to lie at the following positions: −0.2 ppm, H(5); −0.2 ppm, H(6); −0.9 ppm, H(7); 0.2 ppm, CH$_3$. On this basis, the much lower frequency doublet at −0.03 ppm in **1** (0.03 ppm in **3** and **4**) was assigned to H(7).
(13) Huntley, C. M.; Laurenson, G. S.; Rankin, D. W. H. *J. Chem. Soc., Dalton Trans.* **1980**, 954.
(14) Pulham, C. R.; Downs, A. J.; Goode, M. J.; Rankin, D. W. H.; Robertson, H. E. *J. Am. Chem. Soc.* **1991**, *113*, 5149.
(15) Cradock, S.; Koprowski, J.; Rankin, D. W. H. *J. Mol. Struct.* **1981**, *77*, 113.
(16) Boyd, A. S. F.; Laurenson, G. S.; Rankin, D. W. H. *J. Mol. Struct.* **1981**, *71*, 217.
(17) Ross, A. W.; Fink, M.; Hilderbrandt, R. In *International Tables for Crystallography*; Wilson, A. J. C., Ed.; Kluwer Academic Publishers: Dordrecht, The Netherlands, Boston, MA, and London, 1992; Vol. C, p 245.
(18) See Hehre, W.; Radom, L.; Schleyer, P. v. R.; Pople, J. A. *Ab Initio Molecular Orbital Theory*; Wiley: New York, 1986.
(19) Frisch, M. J.; Trucks, G. W.; Head-Gordon, M.; Gill, P. M. W.; Wong, M. W.; Foresman, J. B.; Schlegal, H. B.; Raghavachari, K.; Robb, M. A.; Replogle, E. S.; Gomperts, R.; Andres, J. L.; Binkley, J. S.; Gonzalez, C.; Martin, R.; Fox, D. J.; DeFrees, D. J.; Baker, J.; Stewart, J. J. P.; Pople, J. A. Gaussian Inc., Pittsburgh, PA, 1992.
(20) Huzinaga, S. *Approximate Atomic Wavefunctions*; University of Alberta: Edmonton, Canada, 1971.

Table 2. Structural Parameters for 2,4-(MeCHCH$_2$)B$_4$H$_8$ (Distances in pm, Angles in deg)[a,b]

param		
p_1	r[B(1)−B(2)]	189.1(2)
p_2	$^1/_4${2r[B(2)−C(5)] + r[C(5)−C(6)] + r[C(5)−C(7)]}	158.0(1)
p_3	r[B(2)−C(5)] − $^1/_2${r[C(5)−C(6)] + r[C(5)−C(7)]}	6.3(f)
p_4	r[C(5)−C(6)] − r[C(5)−C(7)]	2.6(f)
p_5	r[B−H$_\mu$](mean)	133.3(10)
p_6	r[B(1)−H(1,2)] − r[B(2)−H(1,2)]	−21.0(22)
p_7	r[B−H$_t$](mean)	120.7(20)
p_8	r[B(1)−H(1)] − r[B(2)−H(2)]	−1.0(f)
p_9	r[C−H]	110.0(4)
p_{10}	B(1)B(2)B(3)	54.0(2)
p_{11}	B(1)B(2)B(3)/B(1)B(4)B(3)	100.4(2)
p_{12}	C(6)C(5)C(7)	114.8(12)
p_{13}	C(6)C(5)C(7)/xz	57.4(f)
p_{14}	B(4)B(2)H(2)/xy	124.5(f)
p_{15}	B(3)B(1)H(1)	113.5(f)
p_{16}	B(1)B(2)B(3)/B(1)H(1,2)B(2)	−4.8(f)
p_{17}	C(6)C(5)H(5)	109.5(f)
p_{18}	C(5)C(6)H(6)	111.1(f)
p_{19}	C(5)C(7)H(8)	111.2(f)
p_{20}	C(6)C(5)C(7)H(8)	60.7(f)
p_{21}	C(6)C(5)H(5)/xz	62.1(f)
p_{22}	C(5)C(6)H(6)/xz	58.6(f)
p_{23}	r[C(5)−C(6)] rotation about z	0.5(f)

[a] For definitions of parameters, see the text. [b] Figures in parentheses are the estimated standard deviations. Key: f = fixed.

Table 3. Structural Parameters for 2,4-(MeCHCHMe)B$_4$H$_8$ (Distances in pm, Angles in deg)[a,b]

param		
p_1	r[B(1)−B(2)]	189.3(3)
p_2	$^1/_5${2r[B(2)−C(5)] + r[C(5)−C(6)] + 2r[C(5)−C(7)]}	157.5(1)
p_3	r[B(2)−C(5)] − $^1/_3${r[C(5)−C(6)] + 2r[C(5)−C(7)]}	6.7(f)
p_4	r[C(5)−C(6)] − r[C(5)−C(7)]	2.8(f)
p_5	r[B−H$_\mu$](mean)	133.8(20)
p_6	r[B(1)−H(1,2)] − r[B(2)−H(1,2)]	−19.7(31)
p_7	r[B−H$_t$](mean)	119.8(31)
p_8	r[B(1)−H(1)] − r[B(2)−H(2)]	−1.0(f)
p_9	r[C−H]	110.2(3)
p_{10}	B(1)B(2)B(3)	53.7(3)
p_{11}	B(1)B(2)B(3)/B(1)B(4)B(3)	100.4(3)
p_{12}	C(6)C(5)C(7)	114.3(4)
p_{13}	C(8)C(6)C(5)C(7)	117.5(17)
p_{14}	B(4)B(2)H(2)/xy	124.5(f)
p_{15}	B(3)B(1)H(1)	113.6(f)
p_{16}	B(1)B(2)B(3)/B(1)H(1,2)B(2)	−4.7(f)
p_{17}	C(6)C(5)H(5)	108.8(f)
p_{18}	H(6)C(6)C(5)H(5)	125.1(f)
p_{19}	C(5)C(7)H(7)	111.2(f)
p_{20}	C(6)C(5)C(7)H(7)	60.5(f)
p_{21}	r[C(5)−C(6)] rotation about z	0.8(f)

[a] For definitions of parameters, see the text. [b] Figures in parentheses are the estimated standard deviations. Key: f = fixed.

basis for H. The theoretical chemical shifts have been referenced to BF_3·OEt_2[2a] and are given in the notation "level of the chemical shift calculation//geometry employed". The calculations were performed on IBM-RS/6000 workstations of the Rechenzentrum der Universität Zürich and of the ETH Zürich.

Molecular Model

On the basis of the NMR evidence and the *ab initio* calculations (see below), the molecular models used to generate the atomic coordinates of **1** and **2** were based on the structure established for 2,4-ethanotetraborane[1] but with one hydrogen atom in the ethano bridge replaced by a methyl group in **1** and two *trans* hydrogen atoms replaced by methyl groups in **2**. Throughout the course of the analysis, the B_4C_2 skeleton of both compounds was assumed to have C_2 symmetry. With the origin at the midpoint of B(1)−B(3), and the z axis parallel to the C_2, or pseudo C_2, axis, the molecular models for **1** (C_1 symmetry) and **2** (C_2 symmetry) are described by the parameters listed in Tables 2 and 3; the atom numbering schemes are shown in Figure 1.

2,4-(MeCHCH$_2$)B$_4$H$_8$. The heavy-atom, C_2B_4, skeleton and the carbon atom of the substituent methyl group, C(7), were

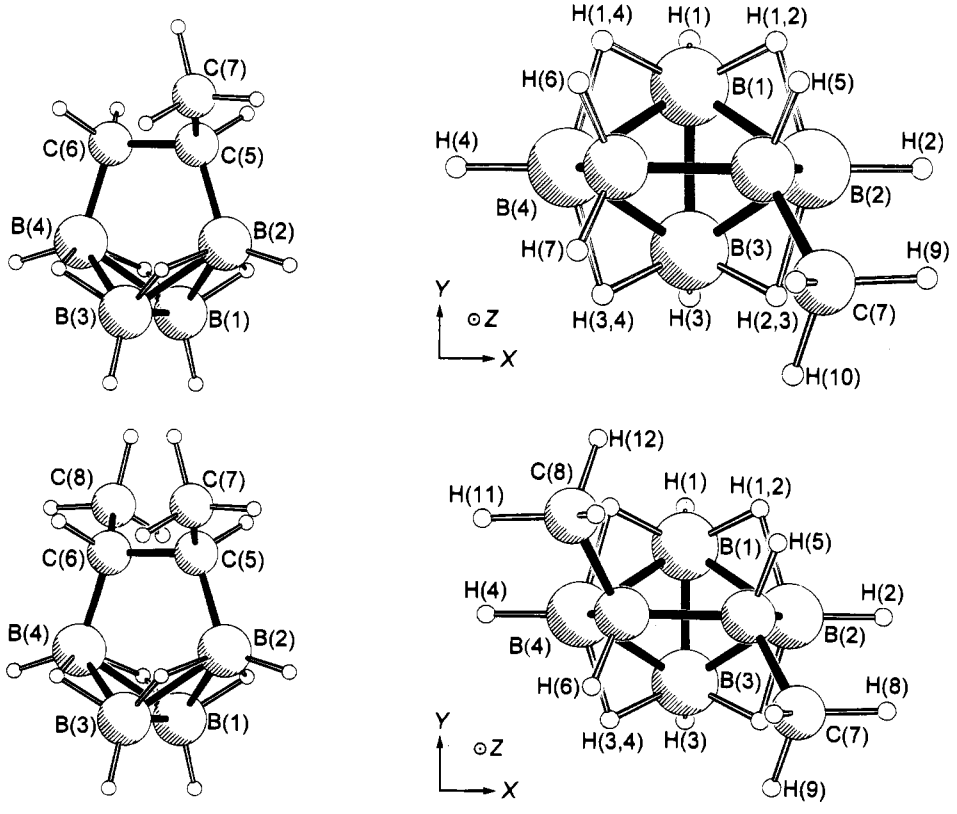

Figure 1. Views of (a) (top) 2,4-(MeCHCH$_2$)B$_4$H$_8$ (**1**) and (b) (bottom) 2,4-(MeCHCHMe)B$_4$H$_8$ (**2**) in the optimum refinements of the electron-diffraction data: (i) (left) perspective view and (ii) (right) view looking down the z-axis.

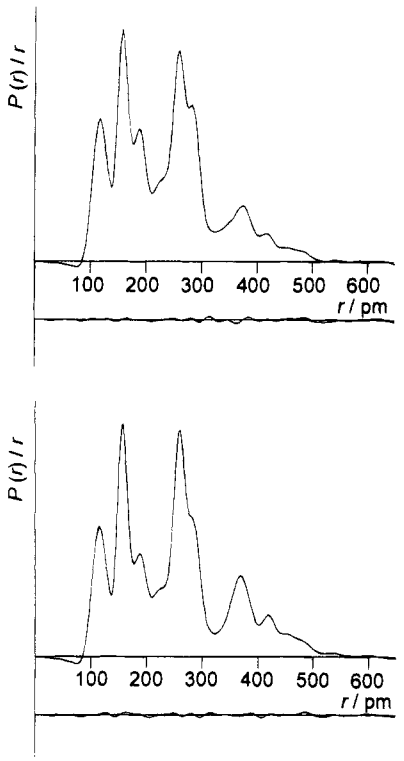

Figure 2. Observed and final weighted difference radial-distribution curves for (a) (top) 2,4-($MeCHCH_2$)B_4H_8 (**1**) and (b) (bottom) 2,4-(MeCHCHMe)B_4H_8 (**2**). Before Fourier inversion the data were multiplied by $s\exp[(-0.00002s^2)/(Z_C - f_C)(Z_B - f_B)]$.

described by eight parameters; these consisted of the distance B(1)−B(2) (p_1), the average of, and the difference between, the B−C and C−C bonded distances (p_2 and p_3), the difference between the C−C bonded distances (p_4), the angle B(1)B(2)B-(3) (p_{10}), the dihedral angle between the planes B(1)B(2)B(3) and B(1)B(4)B(3) (the so-called "butterfly" angle) (p_{11}), the angle C(6)C(5)C(7) (p_{12}), and a rotation of the C(6)C(5)C(7) plane clockwise about C(6)−C(5) out of the xz plane (p_{13}).

The four different types of hydrogen atom were defined by 14 refinable parameters. For the terminal hydrogen atoms attached to boron these consisted of a mean and difference of r[B(1)−H(1)] and r[B(2)−H(2)], p_7 and p_8, the angle B(3)B-(1)H(1), and the angle B(4)B(2)H(2) (calculated for B(1)B(2)B-(3)B(4) coplanar), p_{14}. The bridging hydrogen atoms were defined by three parameters: a mean and a difference of the bond lengths r[B(1)−H(1,2)] and r[B(2)−H(1,2)], p_5 and p_6, and the angle between the planes B(1)B(2)B(3) and B(1)H-(1,2)B(2), p_{16}, defined as positive toward the carbon atoms. The hydrogen atoms attached to carbon were assumed to have identical C−H distances and were then defined by six angle parameters: (a) C(6)C(5)H(5), C(5)C(6)H(6) and C(5)C(7)H-(8); (b) the dihedral angle C(6)C(5)C(7)H(8), p_{20}, measured clockwise about C(7)−C(5) from a position eclipsing C(5)−C(6); (c) rotations of the planes C(6)C(5)H(5) and C(5)C(6)H-(6) anticlockwise about C(6)−C(5) out of the xz plane, p_{21} and p_{22}.

The entire CH_2CHMe group was allowed to rotate about the z axis by an angle p_{23}, such that B(1)···C(5) > B(1)···C(6) for a positive rotation.

2,4-(*trans*-MeCHCHMe)B_4H_8. The model was essentially similar to that for **1** but with the assumption of C_2 symmetry. The major difference was that the two methyl carbon atoms and the two hydrogen atoms of the butyl group were defined using the dihedral angles C(8)C(6)C(5)C(7) and H(6)C(6)C-(5)H(5), p_{13} and p_{18}, respectively.

Table 4. Interatomic Distances (r_a/pm) and Amplitudes of Vibration (u/pm) for 2,4-($MeCHCH_2$)B_4H_8[a-c]

		dist	amplitude
r_1	B(1)−B(2)	189.1(2)	8.2(3)
r_2	B(1)−B(3)	171.6(8)	7.3 (tied to u_1)
r_3	B(2)−C(5)	161.2(9)	6.4(f)
r_4	C(5)−C(6)	156.2(9)	4.9(f)
r_5	C(5)−C(7)	153.6(9)	4.5(f)
r_6	B(1)−H(1)	120.2(20)	8.5(f)
r_7	B(2)−H(2)	121.2(20)	8.5(f)
r_8	B(1)−H(1,2)	122.8(19)	8.5(f)
r_9	B(2)−H(1,2)	143.8(9)	11.5(f)
r_{10}	C(7)−H(8)	110.0(4)	9.0(5)
r_{11}	B(2)···B(4)	258.9(6)	6.9(3)
r_{12}	B(2)···C(6)	257.7(2)	
r_{13}	B(2)···C(7)	257.3(11)	
r_{14}	C(6)···C(7)	261.0(17)	
r_{15}	B(1)···C(6)	285.1(4)	8.4(3)
r_{16}	B(1)···C(5)	285.5(4)	
r_{17}	B,C···H (two bond)	213−287	11.0(f)
r_{18}	B(2)···H(7)	333.9(4)	14.0(13)
r_{19}	B(1)···H(6)	335.1(5)	
r_{20}	B(1)···H(5)	330.1(5)	
r_{21}	B(2)···H(6)	333.3(4)	
r_{22}	C(7)···H(2)	305.1(30)	
r_{23}	C(7)···H(6)	332.1(16)	
r_{24}	B,C···H (three bond)	263−378	14.0(f)
r_{25}	B(3)···C(7)	365.9(6)	11.5(10)
r_{26}	B(4)···C(7)	373.4(12)	
r_{27}	C(6)···H(3)	402.1(17)	14.5(30)
r_{28}	C(6)···H(1)	401.6(17)	
r_{29}	B(1)···C(7)	417.9(4)	10.5(17)
r_{30}	C(7)···H(3)	468.2(14)	16.3(61)
r_{31}	C(7)···H(4)	482.0(19)	
r_{32}	C(7)···H(1,4)	436.1(9)	
r_{33}	B(1)···H(9)	461.4(13)	
r_{34}	B(1)···H(10)	433.8(6)	
r_{35}	B(1)···H(8)	499.7(7)	
r_{36}	B(4)···H(9)	456.0(6)	
r_{37}	B(4)···H(8)	429.2(18)	
r_{38}	B(3)···H(9)	416.7(4)	
r_{39}	B(3)···H(8)	457.2(10)	
r_{40}	B,C···H (four bond)	338−532	18.0(f)

[a] For atom numbering scheme, see Figure 1. Values in parentheses are the estimated standard deviations. [b] H···H nonbonded distances were also included in the refinements, but are not listed here; amplitudes of vibration were fixed in the range 14−20 pm. [c] Key: f = fixed.

Results

Refinement of the Structures. The radial-distribution curves for **1** and **2** are similar, showing six distinct peaks at distances near 121, 163, 190, 265, 375, and 417 pm together with two shoulders at *ca.* 225 and 287 pm (Figure 2). The peaks at $r <$ 200 pm correspond to scattering from bonded atom pairs; the B−H (terminal and short bridging) and C−H bonds contribute to the peak at *ca.* 121 pm, while the peak at *ca.* 163 pm has contributions from the two types of C−C, the B−C, and the long B−H_b bonded distances. The feature at *ca.* 190 pm represents scattering from the two types of B−B distances. The B(2)···C(7), B(2)···C(6), B(2)···B(4), and C(6)···C(7) nonbonded pairs contribute mainly to the peak at *ca.* 265 pm, and the nonbonded pairs B(1)···C(5) and B(1)···C(6) are identified with the shoulder at 287 pm; both are augmented by two-bond B···H and C···H distances. The shoulder at *ca.* 225 pm represents scattering from two-bond C···H and B···H atom pairs. The peak at 375 pm is due to scattering from B(3)···C-

Table 5. Interatomic Distances (r_a/pm) and Amplitudes of Vibration (u/pm) for 2,4-(MeCHCHMe)B_4H_8[a-c]

		dist	amplitude
r_1	B(1)−B(2)	189.3(3)	8.6(4)
r_2	B(1)−B(3)	171.2(9)	7.7 (tied to u_1)
r_3	B(2)−C(5)	161.5(11)	6.4(f)
r_4	C(5)−C(6)	156.7(11)	4.9(f)
r_5	C(5)−C(7)	153.9(11)	4.5(f)
r_6	B(1)−H(1)	119.3(31)	8.5(f)
r_7	B(2)−H(2)	120.3(31)	8.5(f)
r_8	B(1)−H(1,2)	124.0(34)	8.5(f)
r_9	B(2)−H(1,2)	143.7(13)	11.0(f)
r_{10}	C(7)−H(7)	110.2(3)	8.6(4)
r_{11}	B(2)···B(4)	259.6(7)	6.5(2)
r_{12}	B(2)···C(6)	258.3(2)	
r_{13}	B(2)···C(7)	256.8(11)	
r_{14}	C(6)···C(7)	260.9(6)	
r_{15}	B(1)···C(6)	285.4(5)	8.3(3)
r_{16}	B(1)···C(5)	286.1(5)	
r_{17}	B(2)···H(5)	221.2(3)	12.1(7)
r_{18}	C(6)···H(5)	218.6(3)	
r_{19}	C(5)···H(8)	219.3(3)	
r_{20}	B(7)···H(5)	215.7(9)	
r_{21}	B,C···H (two bond)	235−286	11.0(f)
r_{22}	B,C···H (three bond)	271−402	14.0(f)
r_{23}	B(3)···C(7)	363.8(13)	13.2(6)
r_{24}	B(4)···C(7)	372.3(4)	
r_{25}	C(7)···C(8)	371.2(23)	
r_{26}	B(1)···C(7)	417.2(7)	9.5(10)
r_{27}	B(1)···H(8)	461.7(8)	17.3(18)
r_{28}	B(1)···H(7)	499.6(6)	
r_{29}	B(4)···H(8)	455.7(4)	
r_{30}	C(7)···H(3)	464.9(34)	
r_{31}	C(7)···H(4)	479.9(30)	
r_{32}	C(7)···H(11)	458.3(20)	
r_{33}	B(1)···H(10)	455.1(13)	
r_{34}	B,C···H (four bond)	334−530	18.0(f)

[a] For atom numbering scheme see Figure 1. Values in parentheses are the estimated standard deviations. [b] H···H nonbonded distances were also included in the refinements, but are not listed here; amplitudes of vibration were fixed in the range 14−23 pm. [c] Key: f = fixed.

(7) and B(4)···C(7) nonbonded pairs together with C(7)···C(8) pairs for **2**. The peak at 417 pm consists of scattering from B(1)···C(7).

Of the nine parameters defining the positions of the heavy atoms (Tables 2 and 3), it was possible to refine five for **1** and six for **2**. For both sets of refinements, the effects of correlation negated the possibility of refining p_3 and p_4 and also p_{13} in the analysis of **1**. All of the parameters pertaining to B−H and C−H bonded distances were refined simultaneously with the exception of $\Delta(B-H_t)$, p_8. However, the estimated standard deviations for the B−H parameters are large and these hydrogen atom positions are subsequently poorly defined. Moreover, it was not possible to refine any of the angle parameters relating to the positions of the hydrogen atoms; such attempts resulted in either unacceptably large esds or unstable refinements. Such parameters were fixed at values suggested by the *ab initio* study. In addition, it proved possible to refine 8 amplitudes of vibration in the final refinement of **1** and 7 for **2**.

Distortion of the methylethano and dimethylethano groups about their respective pseudo C_2 and C_2 axis was also explored. For **2**, p_{21} refined to a value in the range −1.0(5) to −4.2(6)° depending upon the refinement conditions; the R_G value improved by *ca.* 0.01 during the course of these refinements. However, the resulting structure possessed a B(1)−B(3) bonded

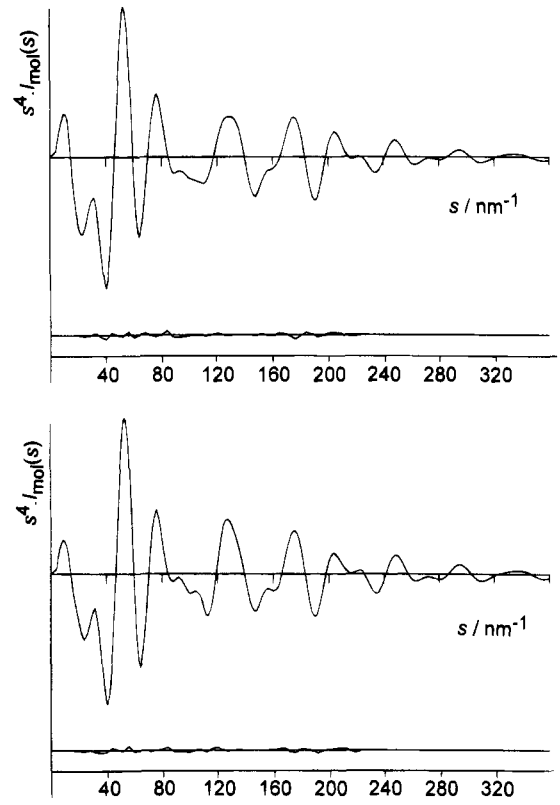

Figure 3. Observed and final weighted difference combined molecular-scattering intensity curves for (a) (top) 2,4-(MeCHCH$_2$)B_4H_8 (**1**) and (b) (bottom) 2,4-(MeCHCHMe)B_4H_8 (**2**). Theoretical data are shown for the regions 0−20 and 224−360 nm^{-1} for which no experimental data are available.

distance of 175.7(13) pm; this is considerably longer than the value determined experimentally for any other tetraborane(10) derivative.[1,21] For **1**, refinement of p_{23} resulted in a twist angle of −3.0(6)°. It was, however, necessary to reduce the number of simultaneously refining amplitudes by two in order to obtain a stable refinement. Clearly, the effects of correlation make any conclusions regarding the ethano twist angle tenuous; at most, the GED analysis suggests that this angle is small. In the final refinements the twist angles were set therefore at the *ab initio* values, both of which were less than 1°.

The relatively low symmetry of the molecules, allied to the lack of any rigorously based vibrational assignment, ruled out the possibility of applying shrinkage corrections. However, it has been possible to calculate the harmonic frequencies of ethanotetraborane, 2,4-(CH$_2$CH$_2$)B_4H_8, *ab initio* at the MP2/6-31G* level.[22] The a_2 mode, describing a twisting motion of the C_2H_4 moiety about the C_2 axis, is predicted to occur at *ca.* 156 cm^{-1}. The electron-diffraction analysis of 2,4-(CH$_2$CH$_2$)-B_4H_8 assumed a C_{2v} geometry in the final refinements but explored the twisting of the C_2H_4 group *via* refinements in which an extra parameter, p_{16}, allowed for a distortion along this a_2 coordinate.[1] The refined value of 2.1(16)° was ascribed to a shrinkage effect and is in keeping with the calculated low frequency of the a_2 mode. It has not been possible to calculate the frequencies of the analogous ethano twisting modes of **1** and **2**; the low symmetry of these structures makes such computations prohibitively expensive. It is, however, likely that

(21) Dain, C. J.; Downs, A. J.; Laurenson, G. S.; Rankin, D. W. H. *J. Chem. Soc., Dalton Trans.* **1981**, 472.
(22) As reported in ref 1, the C_{2v} form of 2,4-(CH$_2$CH$_2$)B_4H_8 is a transition state at Hartree−Fock levels. Our new results confirm that this structure is a true minimum at the electron-correlated MP2/6-31G* level, as no imaginary frequencies are computed.

Table 6. Least-Squares Correlation Matrix (×100) for (a) 2,4-(MeCHCH$_2$)B$_4$H$_8$ and (b) 2,4-(MeCHCHMe)B$_4$H$_8$[a]

(a)

p_6	p_7	p_9	p_{11}	p_{12}	u_1	u_{12}	u_{29}	u_{30}	k_2	
				-56		59				p_2
63	-81	53	-64							p_5
	-74		-79							p_6
		-58	79				60			p_7
					67					p_{10}
				-59			51			p_{11}
						-67				p_{12}
									52	u_{12}
									55	u_{15}
								63		u_{27}
									62	k_1

(b)

p_2	p_5	p_6	p_7	p_9	p_{11}	p_{12}	p_{13}	u_1	u_{14}	u_{19}	u_{23}	u_{26}	u_{27}	k_2	
58							64			-53					p_1
	66						80	-50		-65					p_2
		78	-90	52	-71		63	-50		-70		-53	63		p_5
			-85		-85	54					52	-53	54		p_6
				-53	81	-55				54	-50	63	-65		p_7
											-68	57			p_{11}
								-52		-68					p_{13}
										65					u_1
										-53					u_{14}
									55						u_{15}
														51	k_1

[a] Only elements with absolute values >50 are shown. k is a scale factor.

such frequencies will be similar to that for 2,4-(CH$_2$CH$_2$)B$_4$H$_8$ and that a shrinkage effect is to be expected. The experimental values of p_{21}, for **1**, and p_{23}, for **2**, discussed above must, at leat in part, be a result of this shrinkage.

The success of the final refinements, for which $R_G = 0.056$ ($R_D = 0.049$) for **1** and $R_G = 0.047$ ($R_D = 0.045$) for **2**, may be assessed on the basis of the difference between the experimental and calculated radial-distribution curves (Figure 2). Figure 3 offers a similar comparison between the experimental and calculated molecular-scattering curves while the structural details and vibrational amplitudes of the optimum refinements are listed in Tables 4 and 5. The most significant elements of the least-squares correlation matrices are shown in Table 6.

***Ab Initio* and IGLO Calculations.** The structures of **1** and **2** were optimized in C_1 and C_2 symmetry, respectively, at the HF/3-21G level. At this level, the structure of **1** was optimized to a very asymmetric geometry with B−B distances of 177.8 pm (hinge−hinge) and 210.4, 210.4, 194.5, and 179.7 pm (hinge−wing). A frequency calculation at the same level showed the C_2 geometry for **2** to be a transition state, one imaginary vibrational frequency being calculated. This is consistent with the results for the parent compound 2,4-(CH$_2$-CH$_2$)B$_4$H$_8$[1] for which a "false minimum", *i.e.* a symmetry lower than C_{2v}, is obtained at Hartree−Fock levels and electron correlation effects need to be included for a correct description of the potential-energy surface.[2a,22,23] Reoptimization of **1** and **2** at the correlated MP2/6-31G* level resulted in the C_2 geometry being favored for **2** and a much less asymmetric geometry being found at the potential-energy minimum for **1**. The results are given in Tables 7 and 8. MP2/6-31G* level frequency calculations could not be performed for **1** and **2** (because of the very large amount of CPU time required), but as for 2,4-(CH$_2$CH$_2$)-B$_4$H$_8$, the MP2/6-31G* geometries are expected to be true minima.

The distortion of the B$_4$C$_2$ framework away from C_{2v} symmetry was calculated to be very small for **1** at the MP2/6-31G* level. The B−B distances spanned the narrow range 185.9−186.6 pm, and the B−C distances differed by only 0.3 pm. Similarly, the long and short B−H$_\mu$ distances differed by only 0.3 and 0.4 pm, respectively. The BCCB dihedral angle optimized to a value of 0.9°, and the differences between the same types of angles, *e.g.* B(1)B(2)B(3) and B(1)B(4)B(3), were less than 1°. Likewise for **2**, in which all B−B distances were calculated to be equal and the same types of B−H$_\mu$ distance

(23) (a) Schleyer, P. v. R.; Gauss, J.; Bühl, M.; Greatrex, R.; Fox, M. A. *J. Chem. Soc., Chem. Commun.* **1993**, 1766. (b) Bühl, M.; Gauss, J.; Hofmann, M.; Schleyer, P. v. R. *J. Am. Chem. Soc.* **1993**, *115*, 12385.

Table 7. *Ab Initio* Optimized Geometry (MP2/6-31G* Level) for 2,4-$(MeCHCH_2)B_4H_8$ (Distances in pm, Angles in deg)[a]

	MP2/6-31G* (r_e)	electron diffraction[b] (r_a)
	Distances	
B(1)−B(2)	186.2[c]	189.1(2)
B(1)−B(3)	171.7	171.6(8)
B(2)−C(5)	160.8[c]	161.2(9)
C(5)−C(6)	155.8	156.2(9)
C(5)−C(7)	153.2	153.6(9)
B(1)−H(1,2)	124.7[c]	122.8(19)
B(2)−H(1,2)	142.7[c]	143.8(9)
B-H_t (mean)	119.2[c]	120.7(20)
C(7)−H(8)	109.6	110.0(4)
	Angles	
B(1)B(2)B(3)	54.9[c]	54.0(2)
B(1)B(2)B(3)/ B(1)B(4)B(3) "butterfly"	101.0	100.4(2)
r[C(5)−C(6)] "twist" about *z*	0.5	0.5(f)

[a] For atom numbering scheme, see Figure 1. [b] f = fixed. Values in parentheses are the estimated standard deviations. [c] Mean value calculated for similar types of bonded distance or angle, *e.g.* B(2)−C(5) = $^1/_2$[B(2)−C(5) + B(4)−C(6)].

Table 8. *Ab Initio* Optimized Geometry (MP2/6-31G* level) for 2,4-$(MeCHCHMe)B_4H_8$ (Distances in pm, Angles in deg)[a]

	MP2/6-31G* (r_e)	electron diffraction[b] (r_a)
	Distances	
B(1)−B(2)	186.1[c]	189.3(3)
B(1)−B(3)	171.7	171.2(9)
B(2)−C(5)	160.8	161.5(11)
C(5)−C(6)	156.0	156.7(11)
C(5)−C(7)	153.2	153.9(11)
B(1)−H(1,2)	124.8[c]	124.0(34)
B(2)−H(1,2)	142.7[c]	143.7(13)
B−H_t (mean)	119.3[c]	119.8(31)
C(7)−H(8)	109.7[c]	110.2(3)
	Angles	
B(1)B(2)B(3)	55.0	53.7(3)
B(1)B(2)B(3)/ B(1)B(4)B(3) "butterfly"	100.9	100.4(3)
r[C(5)−C(6)] "twist" about *z*	0.8	0.8(f)

[a] For atom numbering scheme, see Figure 1. [b] f = fixed. Values in parentheses are the estimated standard deviations. [c] Mean value calculated for similar types of bonded distance or angle, *e.g.* B(1)−H(1,2) = $^1/_2$[B(1)−H(1,2) + B(1)−H(1,4)].

differed by only 0.1 pm. The BCCB dihedral angle was computed to be 1.4°.

Such small differences between the same types of bonded distances and angles cannot be detected experimentally by electron diffraction.[8a] The assumption of C_{2v} symmetry, perturbed only by twisting of the C−C bonds about the C_2 axes, for the C_2B_4 cages in the GED analyses is therefore vindicated.

The structures of the four methylethano derivatives *n*-Pr-$(MeCHCH_2)B_4H_7$ (*n* = 1−4; Pr = *n*-propyl) were fully optimized in C_1 symmetry at the HF/3-21G level, affording relative energies of 9.7, 0.0, 9.3, and 1.2 kJ mol^{-1} for the 1-, 2-, 3-, and 4-isomers, respectively. The geometries of the 2- and 4-isomers were then refined at the correlated MP2/6-31G* level. At this level, the 4-isomer (**4**) is calculated to be 0.2 kJ mol^{-1} higher in energy than the 2-isomer (**3**). Parameters describing the heavy-atom skeletons of **3** and **4** optimized at the MP2/6-31G* level are given in Table 9; atomic coordinates are listed as part of the supplementary material.

The most marked structural effect on substitution of the *exo* hydrogen atom at B(2) in **3** or B(4) in **4** is the lengthening of the adjacent B−B (wing−hinge) bonds relative to **1**, *viz.* > 2 pm at the MP2/6-31G* level. Other changes in the B_4C_2 cage geometry are small; for example, the butterfly angles increase by 0.7 and 0.6° and the BCC angles adjacent to the propyl substituent increase by *ca.* 0.8 and 1.1°, respectively. For both **3** and **4**, the carbon atoms of the propyl groups adopt a near coplanar conformation with B(2) and B(4), the hydrogen atoms

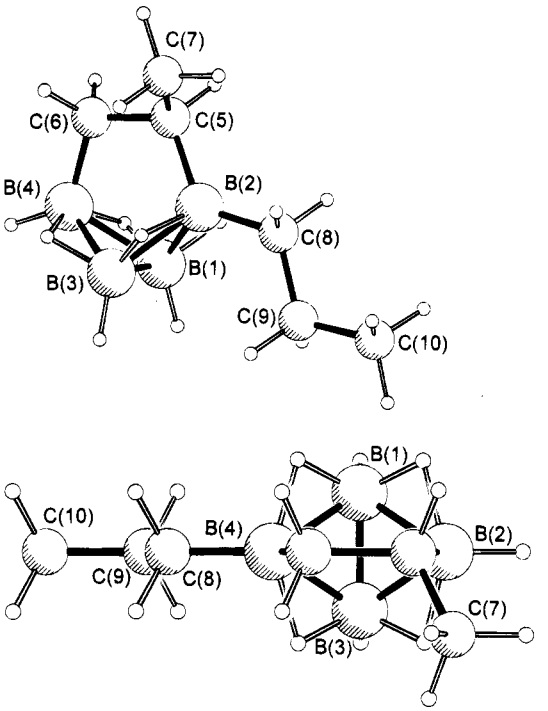

Figure 4. *Ab initio* (MP2/6-31G*) optimized geometries of (a) (top) 2-Pr-2,4-$(MeCHCH_2)B_4H_7$ (**3**) and (b) (bottom) 4-Pr-2,4-$(MeCHCH_2)$-B_4H_7 (**4**).

Table 9. Heavy-Atom Parameters for the *ab Initio* Optimized Geometries (MP2/6-31G* Level) of 2-Pr-2,4-$(MeCHCH_2)B_4H_7$ (**3**) and 4-Pr-2,4-$(MeCHCH_2)B_4H_7$ (**4**) (Distances in pm, Angles in deg)

	3 (2-propyl)	**4** (4-propyl)
	Distances	
B(1)−B(2)	188.3	186.0
B(1)−B(4)	186.3	188.6
B(2)−B(3)	188.1	186.0
B(3)−B(4)	186.3	188.6
B(1)−B(3)	172.1	172.1
B(2)−C(5)	161.2	160.9
B(4)−C(6)	160.5	160.7
C(5)−C(6)	155.8	155.7
C(5)−C(7)	153.2	153.2
B(2)−C(8)	159.4	
B(4)−C(8)		159.3
C(8)−C(9)	153.2	153.2
C(9)−C(10)	152.7	152.7
	Angles	
B(1)B(2)B(3)	54.4	55.1
B(1)B(4)B(3)	55.0	54.3
B(1)B(2)B(3)/ B(1)B(4)B(3) "butterfly"	101.6	101.5
C(6)C(5)C(7)	112.2	112.4
C(5)B(2)C(8)	123.7	
C(6)B(4)C(8)		123.8
B(2)C(8)C(9)	116.1	
B(4)C(8)C(9)		116.1
C(8)C(9)C(10)	112.8	112.9
	Torsions	
B(4)C(6)C(5)B(2)	0.3	0.9
B(4)B(2)C(8)C(9)	0.7	
B(2)B(4)C(8)C(9)		0.4
B(2)C(8)C(9)C(10)	0.1	
B(4)C(8)C(9)C(10)		0.1

Table 10. ^{11}B IGLO Results

molecule	level of theory//geometry	$\delta(^{11}B)$/ppm[a] B(2)	B(4)	B(1)	B(3)	rel energy[b,c]/kJ mol^{-1}
2,4-(MeCHCH$_2$)B$_4$H$_8$	II′//MP2/6-31G*	5.2	2.4	−39.4	−40.0	0.0
	II′//GED	7.0	5.0	−39.5	−40.2	6.1
	expt	*4.8*	*2.0*	*−39.6*	*−40.9*	
2,4-(*trans*-MeCHCHMe)B$_4$H$_8$	II′//MP2/6-31G*	4.6	4.6	−39.7	−39.7	0.0
	II′//GED	6.2	6.2	−39.2	−39.2	5.8
	expt	*4.3*	*4.3*	*−40.1*	*−40.1*	
2-Pr-2,4-(MeCHCH$_2$)B$_4$H$_7$	II′//MP2/6-31G*	18.6	0.4	−38.4	−38.9	
	expt	21.9	−1.6	−38.6	−38.9	
4-Pr-2,4-(MeCHCH$_2$)B$_4$H$_7$	II′//MP2/6-31G*	3.3	16.2	−38.3	−38.9	
	expt	1.4	19.5	−38.6	−38.9	

[a] Relative to BF_3·OEt_2. [b] MP2/6-31G* single-point energy of the GED geometries relative to the MP2/6-31G* fully optimized geometries. [c] Partial optimizations of the GED structures at the MP2/6-31G* level in which the heavy-atom skeletons remained fixed but the locations of the hydrogen atoms were permitted to vary ("H-relaxed") gave relative energies of 2.5 and 4.1 kJ mol^{-1} for 2,4-(MeCHCH$_2$)B$_4$H$_8$ and 2,4-(*trans*-MeCHCHMe)B$_4$H$_8$, respectively.

Table 11. Geometrical Parameters for Tetraborane(10) and 2,4-Ethanotetraborane(10) Derivatives (Distances in pm, Angles in deg)[a,b]

param	2,4-(MeCHCH$_2$)B$_4$H$_8$ GED[c]	MP2[c]	2,4-(MeCHCHMe)B$_4$H$_8$ GED[c]	MP2[c]	2,4-(CH$_2$CH$_2$)B$_4$H$_8$ GED[1]	MP2[1]	B$_4$H$_{10}$ GED[21]	MP2[2a]
"butterfly" angle at B(1)B(3)	100.4(2)	101.0	100.4(2)	100.9	100.8(2)	101.1	117.1(7)	117.3
r[B(1)−B(2)]	189.1(2)	186.2[d]	189.3(3)	186.1[d]	189.5(3)	185.9	185.6(4)	183.5
r[B(1)−B(3)]	171.6(8)	171.7	171.2(9)	171.7	172.9(17)	171.3	170.5(12)	171.4
Δr(B−H$_\mu$)[e]	21.0(22)	18.1[d]	19.7(31)	17.8[d]	19.1(13)	18.0	16.9(13)	15.8

[a] GED = electron diffraction of the vapor; MP2 = theoretical optimization at the MP2/6-31G* level. [b] Values in parentheses are the estimated standard deviations. [c] This work. [d] Mean value calculated for similar types of bonded distance. [e] $\Delta r(B-H_\mu) = r[B(2)-H(1,2)] - r[B(1)-H(1,2)]$.

on adjacent carbon atoms being staggered. The BCC angle in the propyl group is 116.1° in both compounds.

The experimental (GED for **1** and **2**) and theoretical (MP2/6-31G* level for **1**−**4**) geometries were used to calculate NMR chemical shifts using the IGLO method. The calculated values, II′//GED and II′//MP2/6-31G*, are given in Table 10 together with the experimental values.

Discussion

Tetraborane(10) reacts with propene and *trans*-2-butene to give 2,4-(methylethano)tetraborane(10), 2,4-(MeCHCH$_2$)B$_4$H$_8$ (**1**), and 2,4-(*trans*-dimethylethano)tetraborane(10), 2,4-(*trans*-MeCHCHMe)B$_4$H$_8$ (**2**), respectively, as the major volatile products. In the latter reaction, 2,4-(*cis*-MeCHCHMe)B$_4$H$_8$ is not formed, although the reaction of *cis*-2-butene with B$_4$H$_{10}$ does produce the *cis*-isomer.[24] The formation of **2** is thus thought to proceed *via* the simultaneous interaction of the B(2) and B(4) wing-tip atoms of the {B$_4$H$_8$} reactive intermediate with the C=C atoms of the butene. These observations confirm the concerted reaction mechanism for the reaction of tetraborane(10) with ethene as proposed by Williams and Gerhart.[25]

The presence of 2-Pr- and 4-Pr-2,4-(MeCHCH$_2$)B$_4$H$_7$, **3** and **4**, in the synthesis of **1** indicates that hydroboration of the propene is occuring during the formation of the ethanotetraborane cage; 2,4-(methylethano)tetraborane(10) does not react with propene.[24] The ethanotetraborane derivatives can be viewed as dialkylboranes with the two *endo*-hydrogen atoms of tetraborane(10) replaced by alkyl groups.[23] In this sense, **3** and **4** represent the first known trialkyltetraboranes.[26]

The analysis of the gas-phase electron-diffraction patterns confirm the spectroscopic evidence that the molecules **1** and **2** have geometries similar to that of tetraborane(10), with the *endo* hydrogen atoms bonded to the "wing" boron atoms, B(2) and B(4), replaced by bridging ethano units, MeCHCH$_2$ and *trans*-MeCHCHMe, respectively. The main structural parameters, together with those derived by the *ab initio* computations (MP2/6-31G*), are given in Table 7 for **1** and Table 8 for **2**. The theoretical values, defining the equilibrium geometry (r_e), are in very good agreement with those refined from the electron-diffraction patterns (r_a).

The experimental and theoretical geometries of **1** and **2** perform well in the IGLO ^{11}B chemical-shift calculations; the maximum deviation from the $\delta(^{11}B)$ experimental data is 3.2 ppm for the GED geometries and 0.9 ppm for the MP2 geometries (see II′//GED and II′//MP2/6-31G* in Table 10). In addition, single-point energy calculations at the MP2/6-31G* level have been performed for the electron-diffraction structures. Experimental borane and carborane geometries have been assessed previously in this way.[1,2a,6,7] The experimental geometries are calculated to be 6.1 kJ mol^{-1} (**1**) and 5.8 kJ mol^{-1} (**2**) higher in energy than the fully optimized theoretical structure. Such "excess energies" are at the lower end of the normal range found for similarly large boranes and carbaboranes.[1,2a,6,7] Further, partial optimizations of the electron-diffraction structures at the MP2/6-31G* level were also undertaken; the heavy-atom skeletons remained fixed, but the locations of the hydrogen atoms were permitted to vary.[27] These so-called "hydrogen-relaxed" GED geometries of **1** and **2** optimized to structures with calculated energies only 2.5 and 4.1 kJ mol^{-1} greater, respectively, than those for the fully optimized theoretical structures. Thus, a major proportion of the "excess energies" calculated for the GED structures is attributable to the positions of the hydrogen atoms.

The geometries of **3** and **4** optimized at the MP2/6-31G* level (Figure 4 and Table 9) are very similar to **1**. The most apparent effect of substitution is an attenuation of the r(B−B) (hinge−wing) distances adjacent to the propyl group. The high-frequency shift of $\delta(^{11}B)$ for the propyl-substituted boron atoms

(24) Fox, M. A.; Greatrex, R.; Nikrahi, A. Unpublished results.
(25) Williams, R. E.; Gerhart, F. J. *J. Organomet. Chem.* **1967**, *10*, 168.
(26) In the synthesis of **2**, NMR and mass spectroscopic analysis of the nonvolatile material remaining in the reaction vessel indicated the presence of compounds analogous to **3** and **4**. Attempts are being made currently to purify these compounds.
(27) See also: McKee, M. L. *J. Phys. Chem.* **1990**, *94*, 435.

in **3** and **4** relative to **1** is reproduced well by the IGLO (II'// MP2/6-31G*) computations (Table 10). Comparison with the theoretical values has allowed an assignment of the experimental ^{11}B NMR chemical shifts.

Table 11 shows a comparison of some structural parameters for **1**, **2**, 2,4-$(CH_2CH_2)B_4H_8$,[1] and B_4H_{10}.[21] While all of the compounds possess a similar B(1)−B(3) "hinge" distance, the ethano derivatives demonstrate the following noteworthy differences to tetraborane(10): (a) a longer B(1)−B(2) "hinge−wing" distance, 4.5−4.9(5) pm (GED); (b) a narrower "butterfly" angle at B(1)B(3), 16.3−16.7(7)° (GED); (c) more asymmetric B−H_μ distances. As has been discussed before,[1] these structural differences arise as a consequence of the interaction of the $\{B_4H_8\}$ intermediate, thought to be formed initially in these syntheses, with an unsaturated hydrocarbon.

It is noteworthy from Table 11 that, for all four compounds, the theoretical r[B(1)−B(2)] distance is optimized to a value >2 pm shorter than is refined experimentally. The differences in the electron-scattering patterns of the compounds make it unlikely that this discrepancy is ascribable to a systematic effect in the experimental analyses. It is possible that there is a slight shortfall in the particular levels employed in the *ab initio* computations, and attempts are being made to identify its source.

In contrast to 2,4-$(CH_2CH_2)B_4H_8$ in which the H atoms of the CH_2-CH_2 group are eclipsed,[1] the equivalent C and H atoms in **1** and **2** are staggered: for **2**, C(8)C(6)C(5)C(7) = 112.7°, H(6)C(6)C(5)H(5) = 125.1°, and C(8)C(6)C(5)H(5) = 6.2° (MP2/6-31G*). Compared to BCH and CCH in 2,4-(CH_2CH_2)-B_4H_8,[1] the BCC(Me) and CCC(Me) angles are slightly wider and the BCH and CCH angles are slightly narrower at the C(5) and C(6) atoms. Such changes are consistent with the tendency for XCC angles to be larger than XCH angles, for example, CCC in propane[28] compared to CCH in ethane.[18] Steric interactions of the methyl groups in **1** and **2** are also relieved by slight twists of the methylethano groups about the z-axis (see Figure 1); these are less than 1° for both derivatives. These observations support the suggestions made by Onak *et al.*[10]

The structures of **1** and **2** are similar to that of the isoelectronic compound 3,4-bis(pentamethylcyclopentadienyl)tricyclo-[3.1.0.0^{2,6}]hexaphosphane, $P_6(C_5Me_5)_2$, which has been determined by X-ray crystallography.[29] By analogy with the ethanotetraborane derivatives, this may be regarded as a P_4 "butterfly" (the bicyclo[1.1.0]tetraphosphane structural element) bonded at the "wing" atoms, P(2) and P(5), to a $P_2(C_5Me)_5$ moiety. The "butterfly" is distorted very slightly from C_{2v} to C_2 symmetry; the "butterfly" angle at *ca.* 115.5° is much wider than is found for **1**, **2**, and the parent $B_4H_8(CH_2)_2$. Also, in contrast to the $MeCHCH_2$ and MeCHCHMe units in **1** and **2**, respectively, the $P_2(C_5Me_5)_2$ moiety is twisted by *ca.* 11° relative to the P(2)···P(5) (wing···wing) vector, presumably because of the greater steric demands of pentamethylcyclopentadienyl compared to methyl groups.

Acknowledgment. We thank the EPSRC for support of the Edinburgh Electron-Diffraction Service, including provision of microdensitometer facilities at the Daresbury laboratory and research fellowships for P.T.B., M.A.F., and H.E.R. We are indebted to Mr. N. K. Mooljee of the Edinburgh University Computing Service for technical assistance during the course of this work. M.B. thanks Prof. Dr. W. Thiel and the Alfried Krupp-Stiftung (Essen, Germany) for support, and we acknowledge Dr. C. van Wüllen and Dr. M. Schindler for the direct version of the IGLO program. We thank the Royal Society for the MSS Data System at Leeds.

Supplementary Material Available: Listings of atomic coordinates for the GED and theoretically optimized geometries (6 pages). Ordering information is given on any current masthead page.

IC941490X

(28) (a) Schleyer, P. v. R. Unpublished calculations. (b) Boese, R.; Bläser, D.; Niederprüm, N.; Nüsse, M.; Brett, W. A.; Schleyer, P. v. R.; Bühl, M.; Hommes, N. J. R. v. E. *Angew. Chem., Int. Ed. Engl.* **1992**, *31*, 314.

(29) Jutzi, P.; Kroos, R.; Müller, A.; Penk, M. *Angew. Chem., Int. Ed. Engl.* **1989**, *28*, 600.